Hindawi
Advances in Materials Science and Engineering
Volume 2022, Article ID 7534935, 16 pages
https://doi.org/10.1155/2022/7534935

Research Article

Impedance Spectroscopy, AC Conductivity, and Conduction Mechanism of Iron(II) Chloride/Polyvinyl Alcohol/ Polyvinylpyrrolidone Polymer Blend

Huda AlFannakh

Department of Physics, College of Science, King Faisal University, P.O. Box 400, Al-Ahsa 31982, Saudi Arabia

Correspondence should be addressed to Huda AlFannakh; halfannakh@kfu.edu.sa

Received 1 December 2021; Revised 28 February 2022; Accepted 22 June 2022; Published 14 July 2022

Academic Editor: Claudio Pettinari

Polymer blend electrolytes have been prepared using the casting technique. The electrolyte is composed of two polymers polyvinyl alcohol (PVA)/polyvinylpyrrolidone (PVP)) with a fixed ratio (50 : 50) loaded with varied ratios of $FeCl_2$ (0.5, 1, and 2 wt.%). The impedance analysis indicates that the AC conductivity increased as the temperature was following the power law. Nyquist plots for pure and blend composite samples present depressed semicircles at all temperatures. The conduction mechanism of the pure blend sample was based on a hopping mechanism, whereas the ionic conduction was applied to the blend composite sample. The activation energy for blend and blend composite samples was determined, and the two activation regions appeared for blend electrolyte samples. The results indicate a significant improvement in the electrical behavior of the polymeric blend (PVA/PVP) by adding a small weight percentage of $FeCl_2$ salt to the blend samples.

1. Introduction

Polymeric blend and polymer blend composites have received considerable attention due to the great diversity in several industrial applications. The electrical conductivity represents one of the basic properties of the polymers and polymers blend, which motivated researchers to improve the electrical conductivity of these materials. Polyvinylpyrrolidone (PVP) is a nontoxic water-soluble polymer and other polar solvents. It was used in several technological and medical applications [1–8]. Polyvinyl alcohol (PVA) represents one of the famous polymers, which has a wide range of applications, such as packing and biomedical and medical applications [9, 10]. It has also some natural characterization, including nontoxicity, chemical resistance biocompatibility, and hydrophilicity. The polymer blend of synthetic polymers such as PVP and PVA is very important for various applications, such as electrochemical devices [3], heat transfer [11], wound healing [12–14], tissue engineering [15, 16], biological medical applications [3, 4], artificial skin [16], and composite membranes [17, 18]. In addition, several attempts have been made to prepare the blends or composite materials based on PVP and PVA doped with other elements [19–22]. Recently, many researchers have concentrated on the enhancement of the electrical behavior of the PVA/PVP blend by doping the blend with different materials [23–25]. They found that PVA and PVP are miscible due to the interaction between the OH group in PVA and the pyrrolidone ring in PVP (proton-accepting carbonyl group) [26].

Moreover, several studies investigated the properties of the PVA/PVP blend and its composites as a function of frequency and temperature [27]. For instance, Yassin [28] investigated the thermal stability and mechanical and electrical properties of PVA/PVP/Ni-Cd composite. Ragab [29] studied the effect of $NiCl_2$ contents on a PVA/PVP blend using FTIR and dielectric spectroscopy. The modification of the PVA/PVP blend using ZnO was also investigated. In addition, Awang et al. [30] examined the ionic conductivity and dielectric and electrochemical properties of a polymer electrolyte, comprising corn starch and sodium iodate. The impedance spectroscopy analysis of these studies showed that the highest ionic conductivity of polymer

electrolyte was obtained at 3 wt.% of $NaIO_3$, which is the highest dielectric constant. They concluded that the electric modulus analysis can reveal a non-Debye pattern behavior. Therefore, it can be inferred that it is possible to apply the prepared films in some potential electrochemical devices, such as sodium batteries. Another study prepared lithium ion that conducts solid polymer blend electrolytes (SPBE) using PVA/PVP polymer blend and the lithium acetate. The study confirmed the complexation between the polymers and salt by applying X-ray diffraction (XRD) and Fourier transform infrared spectroscopy (FTIR). The transference numbers of polymer electrolytes are calculated by Wagner's polarizing technique, which was also confirmed using Bruce–Vincent technique. Veena and Lobo [31] investigated the effect of different mass% of potassium permanganate ($KMnO_4$) on polyvinyl alcohol–polyvinyl pyrrolidone (PVA–PVP) polymeric blend films. These films have been prepared by applying the solution casting technique using varied filler levels (FL), ranging from 0.01 up to 4.70 mass%. The results indicated a major molecular structural modification, involving the conversion of the hydroxyl (OH) group into ketones at higher FLs. The bands showed a clear distortion in the wide OH band, especially at higher FLs of 3.80 and 4.70 mass%. It was noticed that the value of the glass transition temperature (T_g) decreased by adding fillers in the PVA–PVP blend, whereas the thermal stability of the filled samples increased. Yassin [32] studied the dielectric thermal stability of a PVA/PVP blend filled with different weight percentages of lithium perchlorate ($LiClO_4$). They interpreted the conduction mechanism of the prepared sample using Jonscher's double power law. The study also verified the dominance of the resistive nature over the capacitance and that the conduction in the SPE was only produced by the induced ions. In another study, Badawi et al. [33] investigated the mechanical and electrical properties of SnS (0 to 10.0 wt.%) filled with PVP/PVA (50/50) polymeric composite blends. After checking the dynamic mechanical analyzer (DMA), the study revealed that the storage modulus and stiffness of the neat film are doubled via SnS filling.

The study also found that the T_g values of all SnS-filled PVP/PVA blends increased, compared with that of the neat blend. The DC electrical conductivity (σ) of the neat PVP/PVA polymeric blend has also improved by adding SnS filling, which incrementally increased as the concentration level of SnS raised.

Moreover, the addition of sodium fluoride (NAF) to PVA/PVP blend polymer with different weight ratios was investigated [34]. The XRD spectra show a decrease in the degree of crystallinity of the composite. FTIR analysis confirmed the variation of the microstructure of the system. The study found that the AC conductivity of the system increased in terms of frequency and temperature. Ammonium thiocyanate (NH_4SCN) salt-doped PVA/PVP blend polymer was also examined [35]. XRD confirmed the decrease in the degree of crystallinity of the samples. For instance, the glass transition (Tg) for the composite samples decreased, whereas the concentration of NH_4SCN increased. Wagner's polarization technique showed that the charge transfer in these blend films is predominant due to ions. Saleh and Salman [36] studied the thermal conductivity for PVA/PVP polymer blend doped with different weight ratios of $MnCl_2.4H_2O$. They found that both the coefficient of thermal conductivity and glass transition were affected by the addition of $MnCl_2.4H_2O$.

It is clear from the studies that there is a great interest in studying the physical properties of these blends (PVA/PVP) and blend composites. The present study aims to enhance the conduction mechanism and dielectric properties of the PVA/PVP blend by using low loading of $FeCl_2$ salt (0.5 to 3 wt.%). The effect of temperature and frequency on ionic conduction was also investigated.

2. Experimental

2.1. Materials. PVA (86.7–88.7 mol.% hydrolysis, average molecular weight 67,000 g/mol) and PVP (average molecular weight 55,000 g/mol) were supplied by Sigma Aldrich (USA). $FeCl_2$ (98%) was supplied by Sigma Aldrich (China). PVA, PVP, and $FeCl_2$ were used without further purification or treatment. Deionized water was used as the solvent for preparing the polymer solutions.

2.2. Preparation of Polymer Blend Film Composite. Polymer blends of PVA/PVP solutions were prepared at 50/50 weight ratios. An aqueous PVA solution and PVP were prepared by adding the polymer powder to deionized water, followed by heating the solution under magnetic stirring at 80°C for 2 hours. Both polymeric solutions were mixed and left on a magnetic stirrer overnight to form a homogenous PVA/PVP polymer blend. Iron(II) chloride ($FeCl_2$) with different weight percentages were dissolved in 5 ml of deionized water and ultrasonic homogenizer (Hielscher homogenizer 400 W) for 5 minutes. PVA/PVP/$FeCl_2$ solutions at different weight percentages of $FeCl_2$ were made by mixing the polymer blend and $FeCl_2$ solutions (ultrasonicated for 30 minutes at room temperature). The films were obtained by applying a casting technique that used a Petri dish after drying it at room temperature (32°C) for 3 days. The blend composite samples (PVA/PVP/$FeCl_2$) with different $FeCl_2$ weight percentages (0.5, 1, 2, and 3 wt.%) were kept in a glass desiccator with silica gel.

2.3. Samples Characterization. The polymer blend composite samples were characterized by FTIR and AC spectroscopy. FTIR spectra for PVA/PVP blend and PVA/PVP/$FeCl_2$ blend composite sheet were carried out using the single-beam Fourier transform infrared spectrometer (Perkin Elmer Spectrum 400). The FTIR spectra of the samples were obtained in the spectral range of 400–4,000 cm^{-1}. The AC conductivity and impedance spectroscopy were measured using Keithley Instruments 4200 Semiconductor Characterization System (4200-SCS USA) over a frequency ranging from 1 to 1 MHz, and the temperature range was from room temperature up to 150°C. The AC conductivity was calculated using the following relation:

$$\sigma_{ac} = 2\pi f \varepsilon' \varepsilon_0 \tan \delta, \quad (1)$$

where ε_0 and ε' are the dielectric constant of the free space and the material, respectively; f is the frequency of the applied signal across the sample; and tan δ is the loss tangent or dissipation factor.

3. Results and Discussion

3.1. FTIR Characterization. The effect of $FeCl_2$ on the polymer blend was investigated and analyzed using FTIR spectroscopy. Figure 1 illustrates the FTIR spectra for the pure polymer blend (50% PVA: 50% PVP) and the blend composite (with different weight percentages of $FeCl_2$ (0.5, 2, and 3 wt.%)). The main FTIR absorption band positions and their assignments of the prepared samples are listed in Table 1.

The spectrum of $FeCl_2$/PVA/PVP showed peaks at a similar wave number to that of the polymer blend PVA/PVP, suggesting that $FeCl_2$ did not affect the structural characteristics of the blend.

3.2. Impedance Spectroscopy. One of the most important techniques for detecting the dielectric relaxation processes in polymer, polymer blend, and polymer composite is impedance spectroscopy. From the complex impedance analysis and the expected equivalent circuit based on its data, we can get more information about the physical process that takes place inside the material being tested. Figures 2(a), 2(b), 3(a), 3(b), 4(a), 4(b), 5(a), and 5(b) show the frequency dependence of the real and imaginary parts (Z' and Z'') of impedance at different temperatures ranging from 30 to 140°C for PVA/PVP blend and doped samples. It is clear from the figures that both the real and imaginary parts decrease with increasing temperature.

The pure blend sample (PVA/PVP) does not show any significant dependence on temperature for either the behavior of the real part (Z') or the imaginary part (Z'') of impedance. This behavior can be ascribed to the dielectric nature of the blend sample; therefore, this behavior is closer to the capacitive behavior than the used frequency range. The motion of the main chain due to thermal activation is small, and it adds a slight change in the impedance behavior.

It is also noted that blend samples have a different type of behavior than pure samples. At low temperatures, the behavior is similar to that of the capacitive reactance, and the relationship between the impedance and the frequency is a linear relation. This can be attributed to the incapability of the dipoles to orient or respond to the applied frequency. The frequency-independent plateau region increases with temperature, which is related to the DC conductivity of the polymer blend (see Figures 3(a), 4(a), and 5(a)). In the high-frequency region, the capacitive component of the real part of impedance was predominant, and the dependence becomes linear. As the concentration of $FeCl_2$ increases, the high-frequency dispersion (Z'') shifts towards the higher frequency side, and the conductivity increases (see Figures 3(b), 4(b), and 5(b)). This shift of dispersion to high

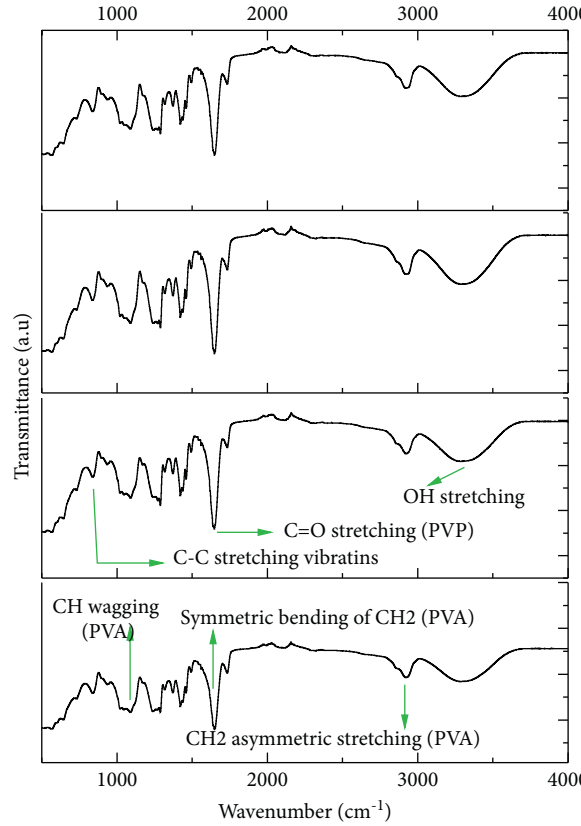

Figure 1: FTIR pattern for 50% PVA: 50% PVP with (a) 0%, (b) 0.5%, (c) 2%, and (d) 3% wt.% $FeCl_2$.

frequency indicates a decrease in the relaxation time that can be attributed to an increase in the electrical conductivity of samples.

Nyquist plots for pure and blend electrolyte samples with different weight percentages (0.5, 1 and 2 wt.%) of $FeCl_2$ are illustrated in Figures 6, 7(a), 7(b), 8(a), 8(b), 9(a), and 9(b), respectively. The plot exhibits depressed semicircles for all samples and at all temperatures. Pure samples did not show a complete semicircle shape due to the insulating nature of the blend and the inability of the charge carriers to move except at high temperatures. This may be attributed to the chain's entanglement. For electrolyte blend and for temperatures higher than 50°C, the semicircles were followed by spikes at the lower frequency side that increased as salt weight percentages and temperatures rose. These results indicate a non-Debye relaxation nature (a single relaxation time) for pure and electrolyte blend samples [49]. The equivalent circuits that represent this depressed semicircle plot include a constant phase element capacitor (CPE) that is parallel to a resistor. This combination was connected in a series with another constant phase capacitive element to represent the shape of the spike at the low-frequency region [50].

Figure 10 shows the effect of $FeCl_2$ weight percentage (concentration) and its temperature on Nyquist plots. It was noted that increasing the temperature and/or $FeCl_2$ weight percentage reduces the diameter of the semicircle, which indicates the active participation of the ionic conductivity through the samples.

Table 1: Absorption band positions and their assignments for PVA/PVP/$FeCl_2$ composite.

Wave number (cm^{-1})	Band assignment	Reference (s)
3,304	OH stretching	[37, 38]
2,929	CH_2 asymmetric stretching deriving from PVA	[38, 39]
1,646	CO stretching deriving from PVP	[40, 41]
1,425	Symmetric bending of CH_2 deriving from PVA	[42, 43]
1,372	CH_2 bending deriving from PVP	[44, 45]
1,290	CH wagging deriving from PVA	[46, 47]
1,090	Stretching vibrations of carbonyl (–C=O) bonds attached to pyrrolidone rings from PVP	[48]
840	CC stretching vibrations deriving from PVA	[47]

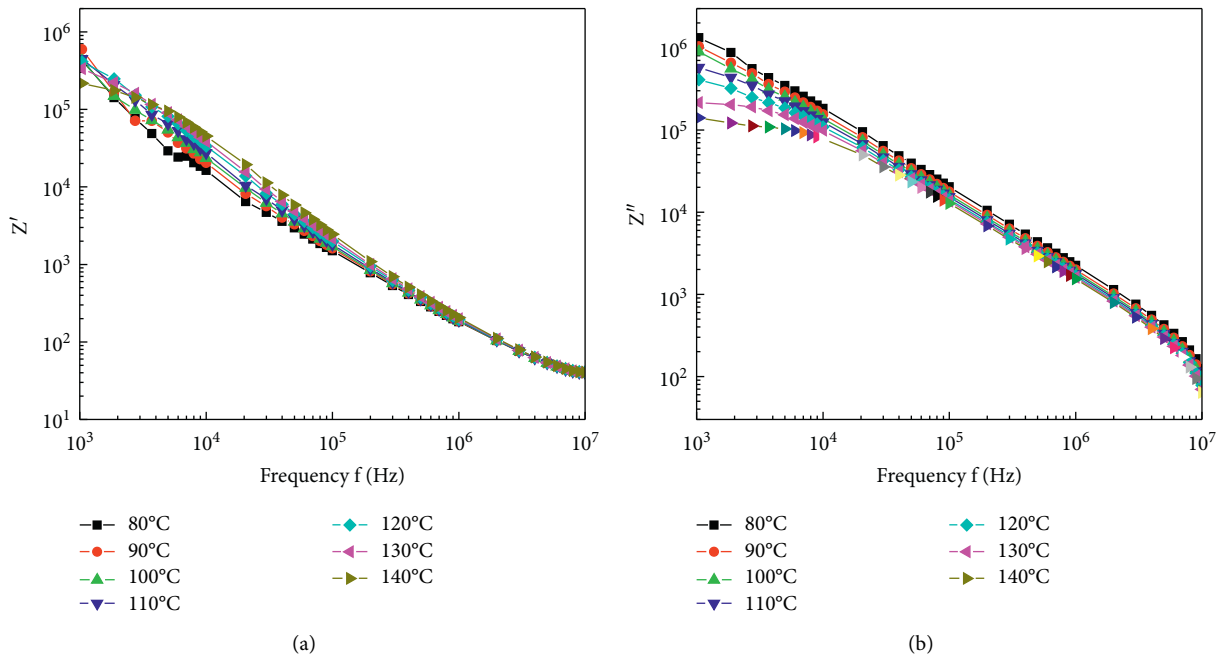

Figure 2: (a) Real part of impedance (Z′) and (b) imaginary part of impedance (Z′) for PVA/PVP polymer blend.

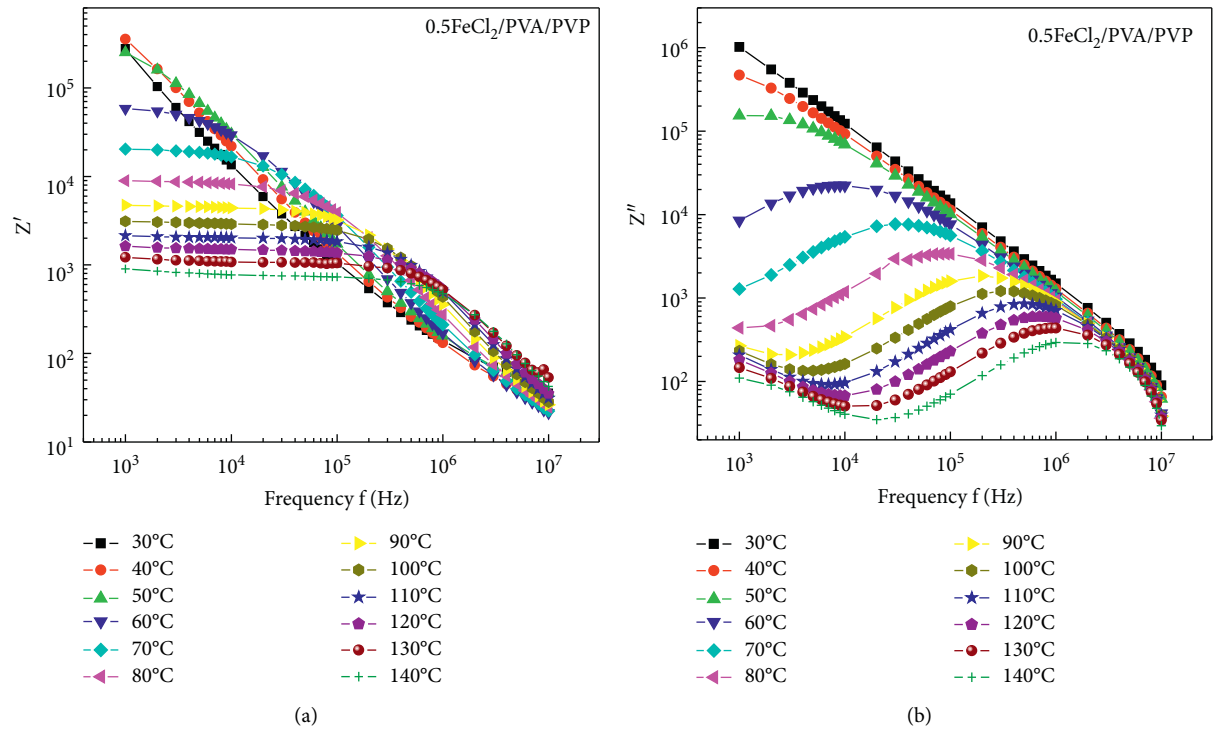

Figure 3: (a) Real part of impedance (Z′) and (b) imaginary part of impedance (Z′) for 0.5 wt.% $FeCl_2$/PVA/PVP polymer blend electrolyte.

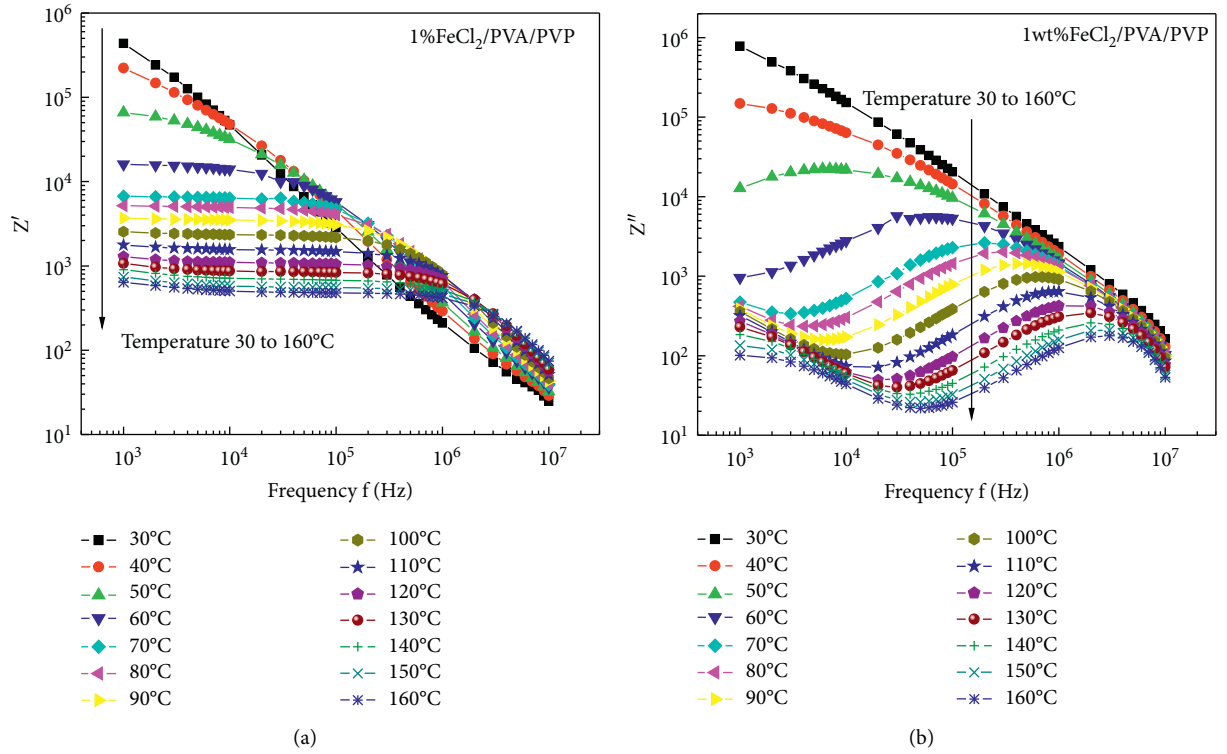

FIGURE 4: (a) Real part of impedance (Z′) and (b) imaginary part of impedance (Z′) for 1 wt.% $FeCl_2$/PVA/PVP polymer blend electrolyte.

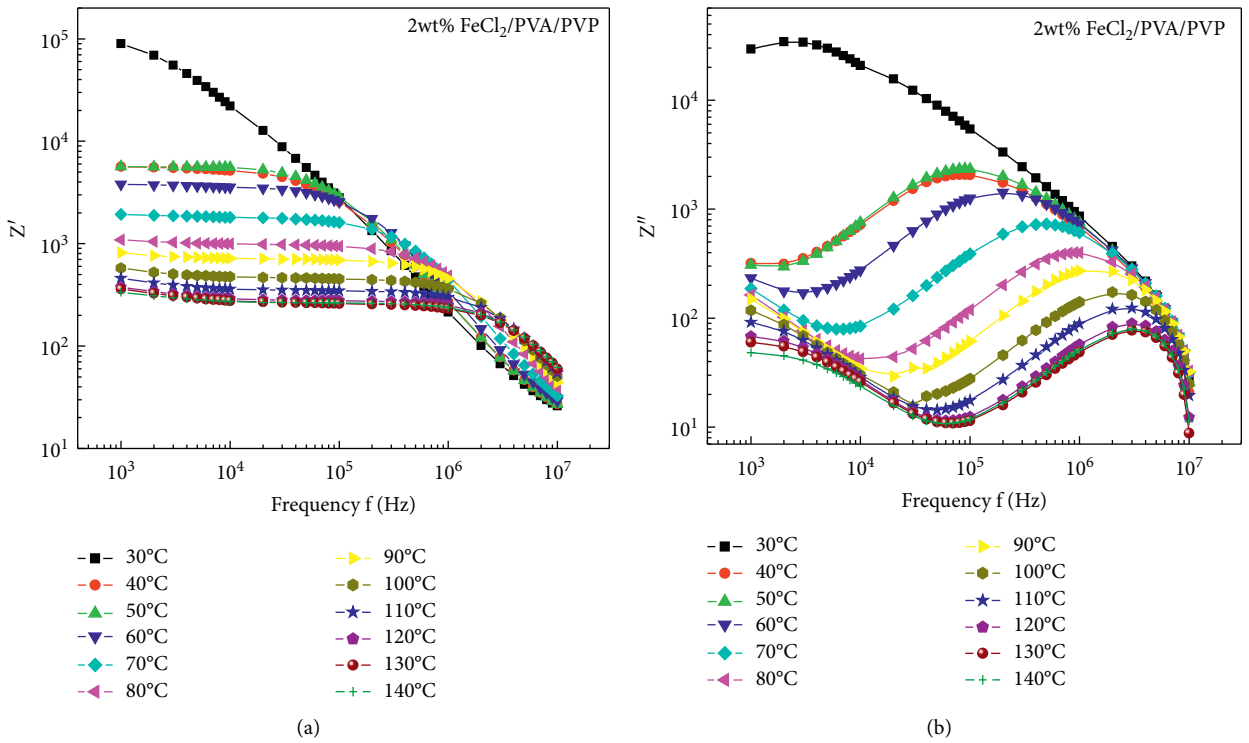

FIGURE 5: (a) Real part of impedance (Z′) and (b) imaginary part of impedance (Z′) for 2 wt.% $FeCl_2$/PVA/PVP polymer blend electrolyte.

3.3. AC Conductivity. Figures 11(a), 12(a), 13(a), and 14(a) illustrate the variation of AC conductivity (σ_{ac}) as a function of frequency and at different temperatures for pure 50 wt.% PVA-50 wt.% PVP blend and doped with 0.5, 1, and 2 wt.% $FeCl_2$. The AC conductivity (σ_{ac}) is found to be temperature and frequency-dependent. AC conductivity behaviors of all

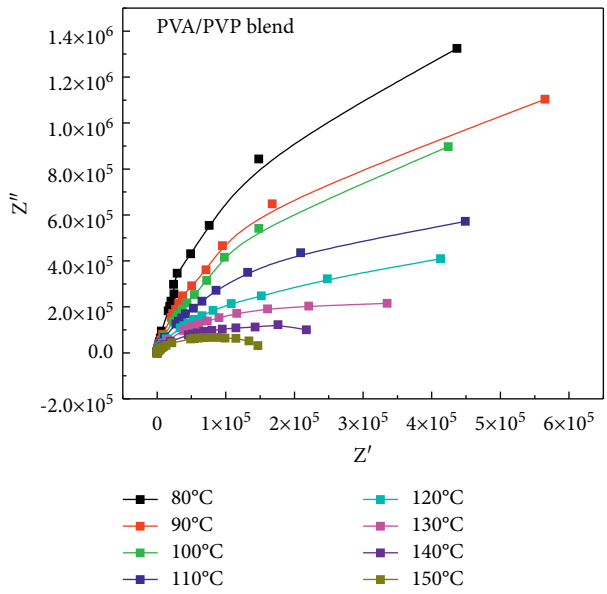

Figure 6: Complex plane plots (Z′-Z″) for PVA/PVP polymer blend at various temperatures.

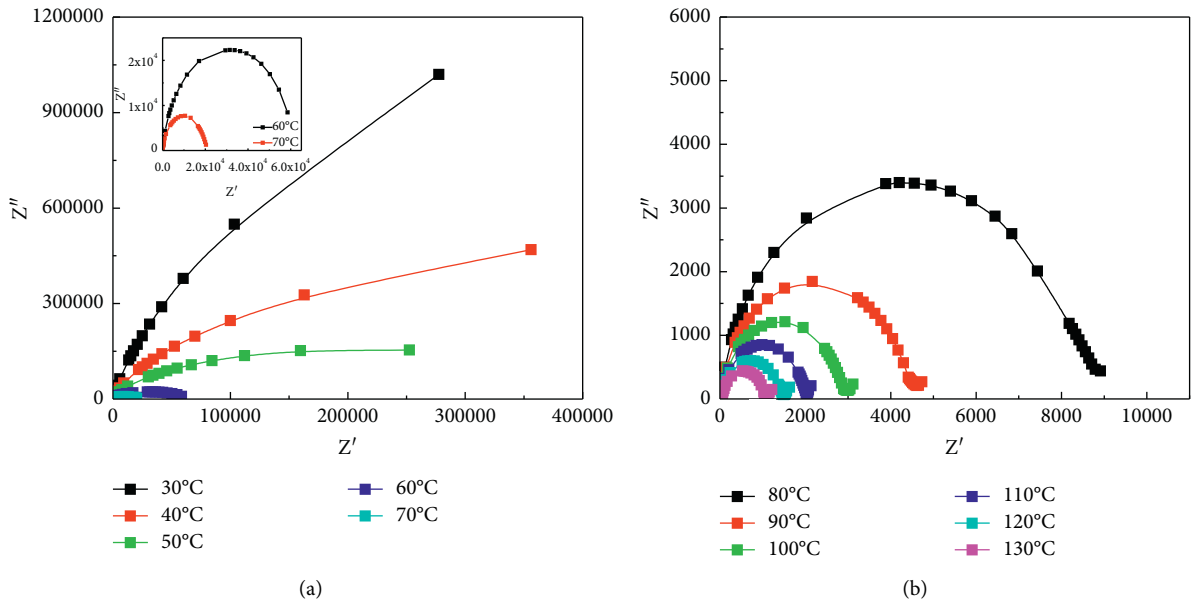

Figure 7: Complex plane plots (Z′-Z″) for 0.5 wt.% $FeCl_2$/PVA/PVP blend composite at various temperatures (a) from 30 to 70°C and (b) from 80 to 130°C.

blend electrolyte samples are characterized by plateau region (frequency-independent) at a higher temperature. This plateau becomes more predominant in higher weight percentages of doped samples (2 wt.%).

For the low-frequency region, σ_{ac} in blend electrolyte samples was frequency independent, especially at a temperature higher than 50°C. This can be attributed to ionic conduction that dominates the AC conductivity that rises as a result of the response of the polymer chains and dipoles to the applied frequencies. For the pure blend sample, it is noticed that the frequency dependence of the AC conductivity continued up to 80 or 90°C, and its increase was attributed to the hopping mechanism [51, 52].

Figures 11(b), 12(b), 13(b), and 14(b) show the variation of log (σ_{ac}) with 1000/T for pure blend, 0.5, 1, and 2 wt.% $FeCl_2$ electrolyte blend samples. It is obvious that the AC conductivity was thermally activated, and the mobility of the charge carrier and charge density increased as the temperature rose. The main chain and the segmental chain motion play an important role in the conductivity behavior of pure and electrolyte samples [52].

The addition of electrolyte to polymer or polymer blend can form complexes with the polymeric chains, which impedes the movement of the chains and makes them require higher energy to contribute to the AC electrical conductivity. This ionic conductivity has the advantage in the active

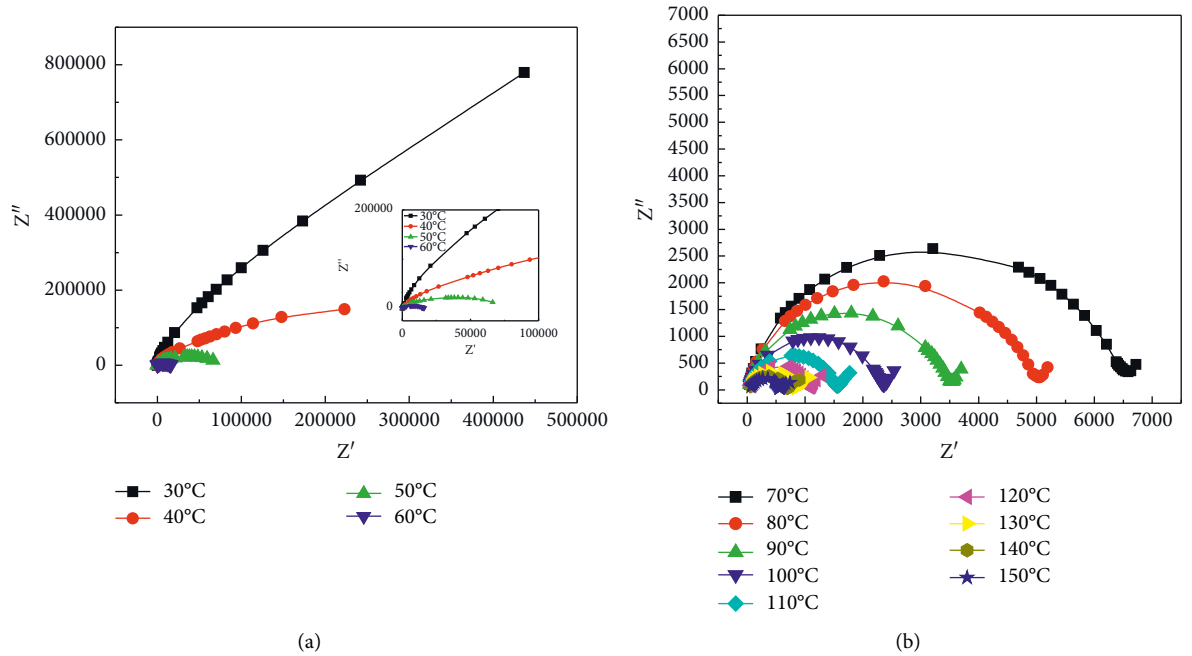

(a) (b)

FIGURE 8: Complex plane plots (Z'-Z'') for 1 wt.% $FeCl_2$/PVA/PVP blend composite at various temperatures (a) from 30 to 60°C and (b) from 70 to 150°C.

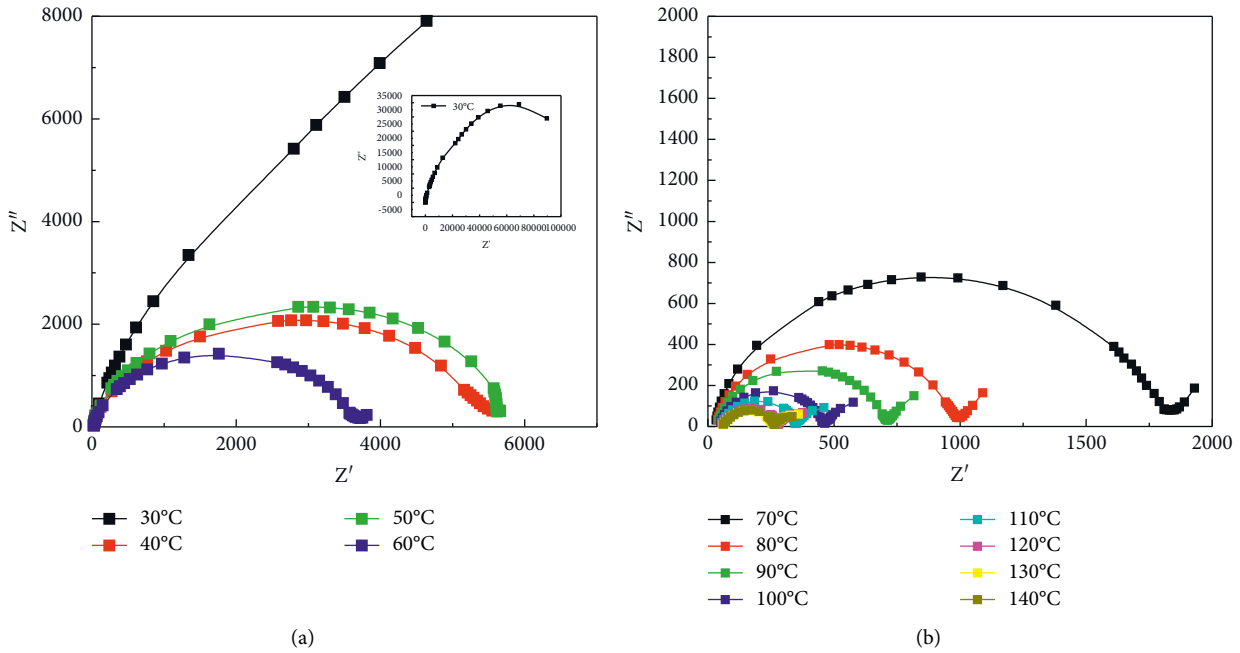

(a) (b)

FIGURE 9: Complex plane plots (Z'-Z'') for 2 wt.% $FeCl_2$/PVA/PVP blend composite at various temperatures (a) from 30 to 60°C and (b) from 70 to 140°C.

participation of the AC electrical conductivity. Occasionally, at small concentrations of salt, the fluid can act as a plasticizer and facilitate the movement of the polymeric chains. From Table 2, it is noted that the electrolyte blend samples have two linear regions. The first was at low temperatures in which the contribution returns to polymer with activation energy in the range from 0.13 to 0.19 eV (greater than pure blend). This region indicates a complex formation between some chains and the ionic liquid. The activation energy in the second region (ionic conduction contribution) was ranging between 0.2 and 0.43 eV. The activation energy decreased as a result of the salt concentration.

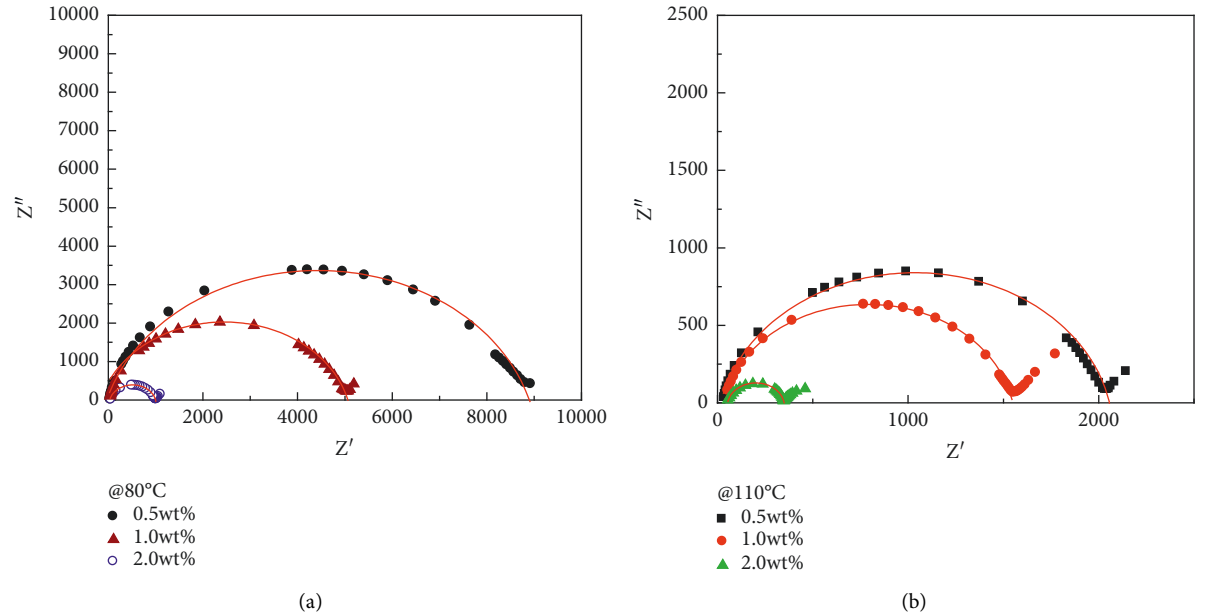

Figure 10: Complex plane plots (Z′ vs. Z″) for PVA/PVP/$FeCl_2$ blend electrolyte samples (a) at 80°C and (b) at 110°C.

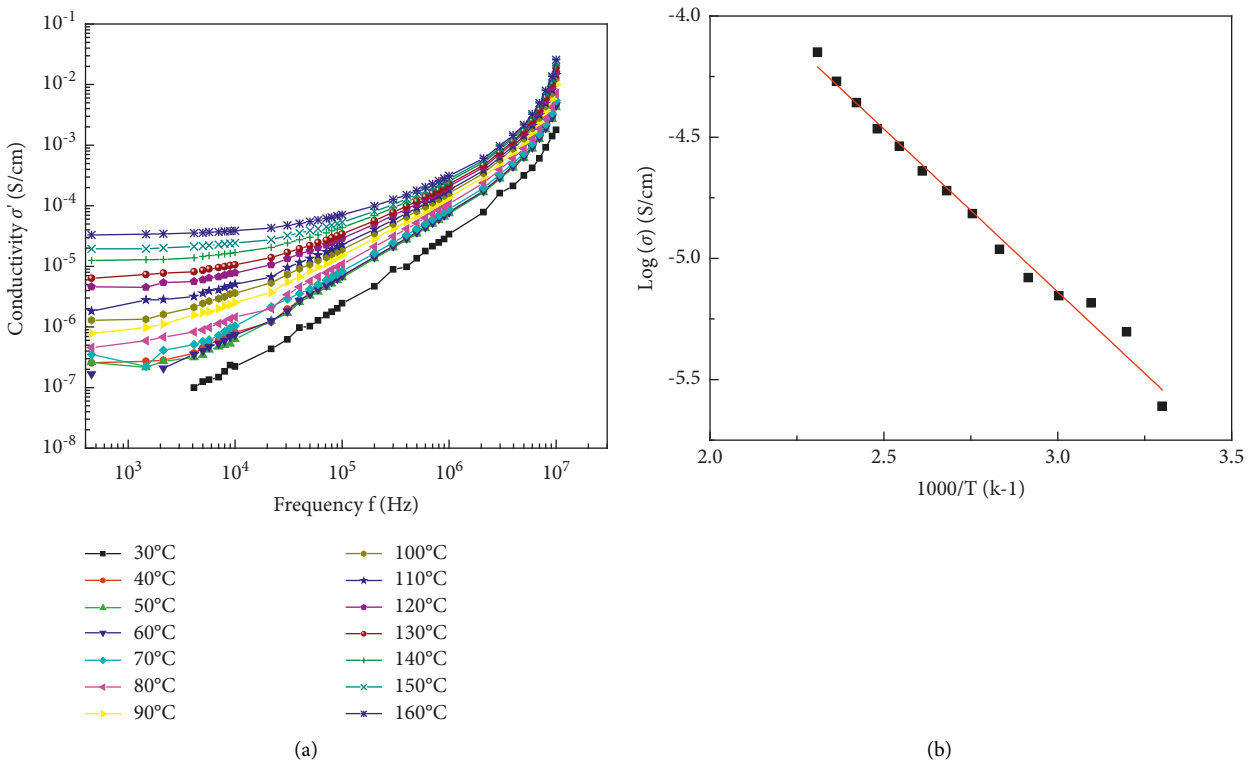

Figure 11: (a) Frequency dependence of AC conductivity at different temperatures and (b) log (σ) versus 1000/T, for pure PVA/PVP blend sample.

Jonscher universal power law can be used to analyze the overall behavior of AC conductivity based on the following equation [53, 54]:

$$\sigma(\omega) = \sigma dc + A\omega n, \quad (2)$$

where $\sigma(\omega)$, σ_{dc}, A, ω, and n are defined as the total conductivity, DC conductivity, constant, angular frequency, and exponent factor, respectively. The dependence of log σ versus log f in the high-temperature region and the dependence of exponent n on temperature are illustrated in Figures 15 and 16 for pure blend and blend composite samples, respectively. The exponent values n were determined by knowing the slope of log σ versus log f relation, which are summarized in Tables 3–6.

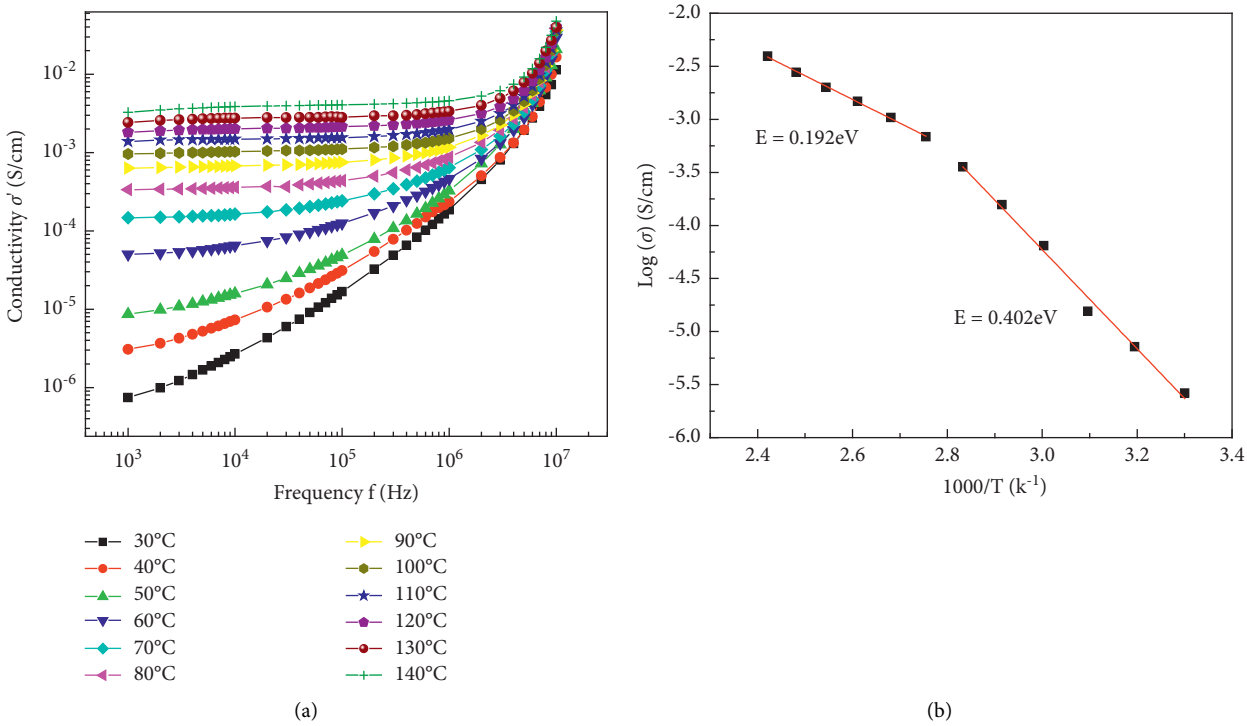

Figure 12: (a) Frequency dependence of AC conductivity at different temperatures and (b) log (σ) versus 1000/T, for 0.5 wt.% $FeCl_2$ PVA/PVP electrolyte blend.

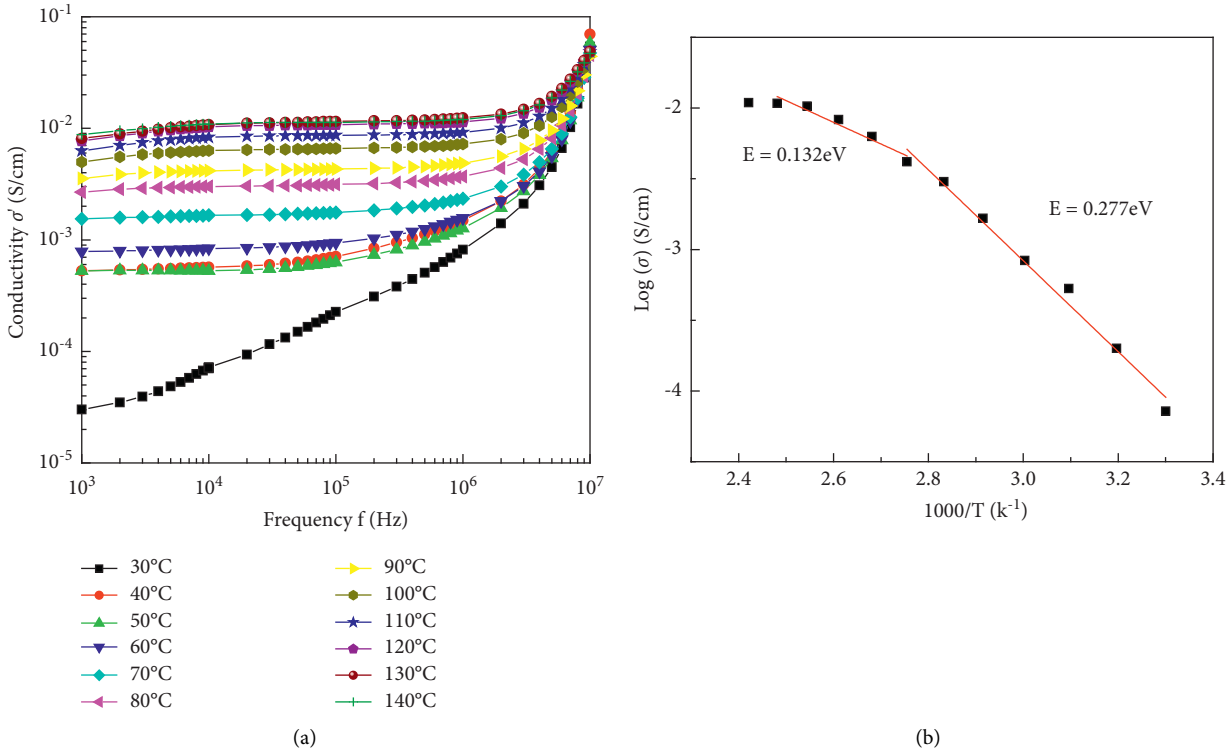

Figure 13 (a) Frequency dependence of AC conductivity at different temperatures. (b) log(·) versus 1000/T, for 1 wt.% FeCl2 PVA/PVP electrolyte blend.

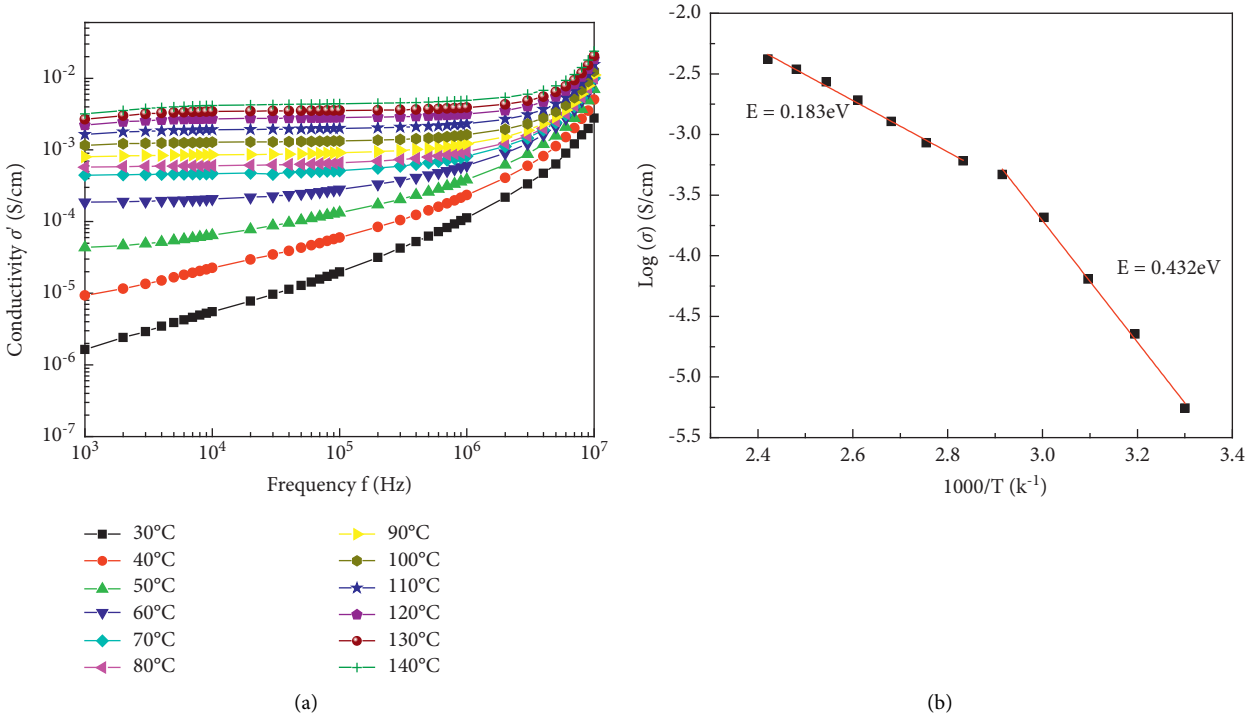

Figure 14: (a) Frequency dependence of AC conductivity at different temperatures and (b) log (σ) versus 1000/T, for 2 wt.% $FeCl_2$ PVA/PVP electrolyte blend.

Table 2: Values of the activation energy for pure and electrolyte PVA/PVP blend sample.

Sample	Activation energy (eV)		R^2
	Region I	Region II	
PVA/PVP	0.12		0.985
PVA/PVP/0.5 wt.% $FeCl_2$	0.402	0.192	0.991 and 0.998
PVA/PVP/2 wt.% $FeCl_2$	0.432	0.183	0.992 and 0.996
PVA/PVP/1 wt.% $FeCl_2$	0.277	0.132	0.922 and 0.942

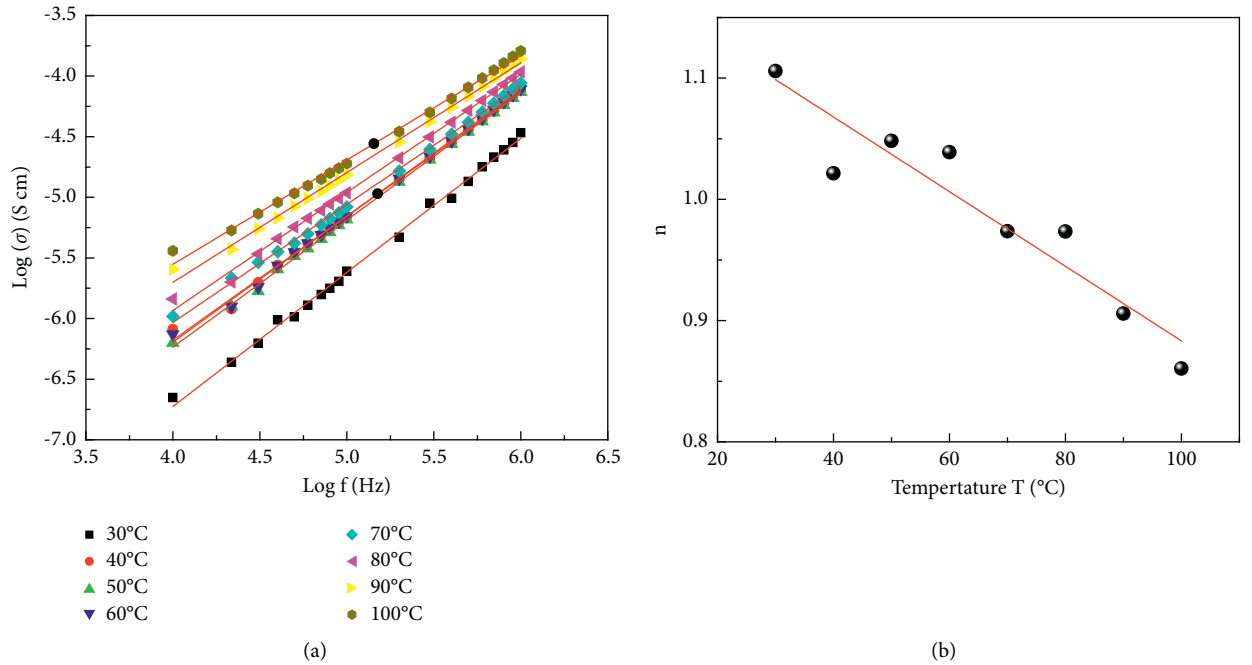

Figure 15: (a, c) log σ versus log f at different temperatures and (b, d) variation of the exponent n against the temperature, for the PVA/PVP blend.

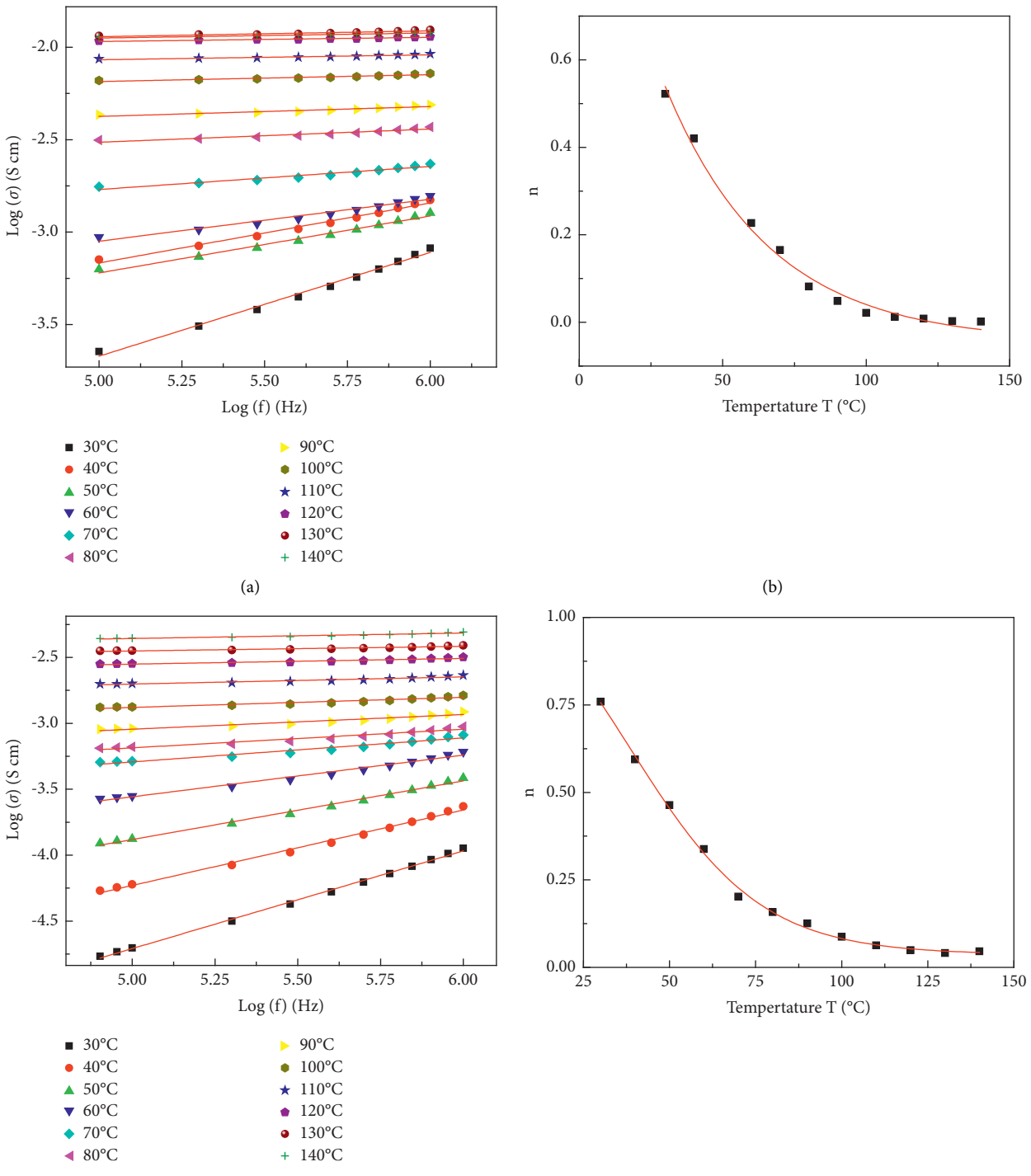

Figure 16: Continued.

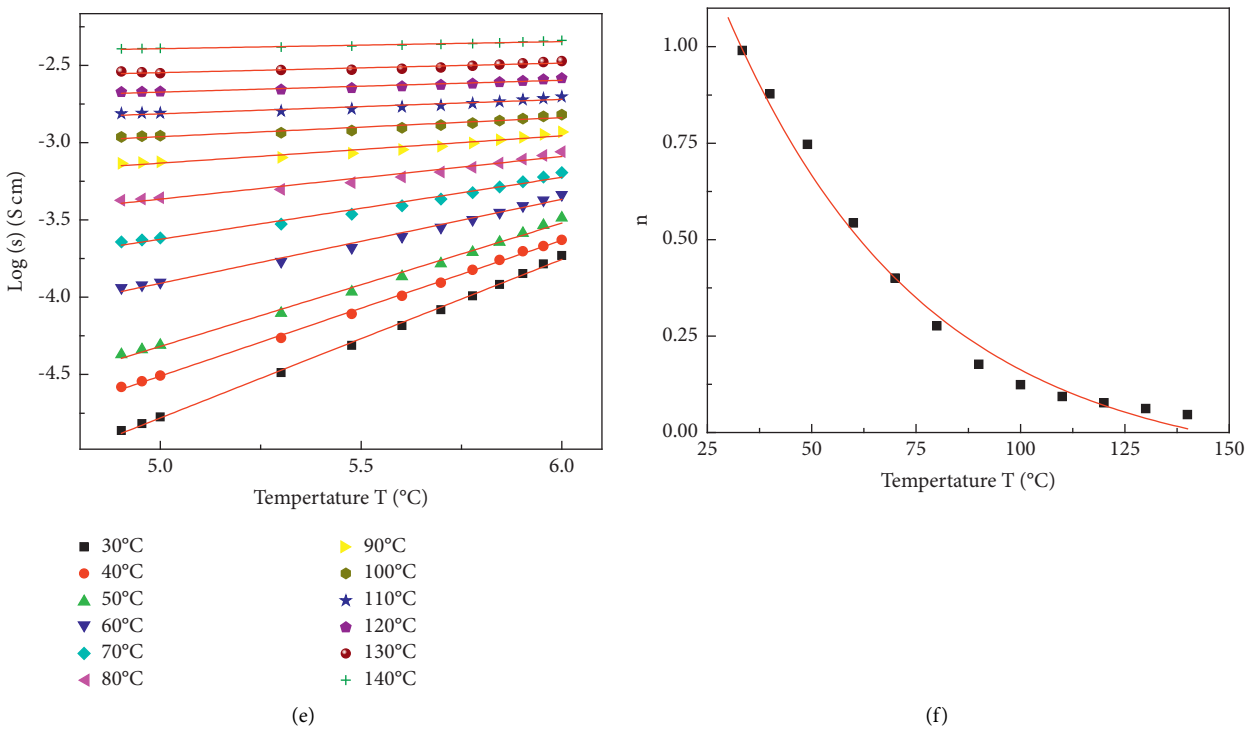

Figure 16: Log σ versus log f in the high-frequency region and the variation of the exponent n against the temperature: (a, b) 0.5 wt.%, (c, d) 1.0 wt.%, and (e, f) 2.0 wt.% $FeCl_2$ PVA/PVP blend electrolyte.

Table 3: Values of the exponent n, coefficient A, and the DC conductivity for pure PVA/PVP blend sample.

T (°C)	Low temperature					
	n	A	σ_{dc}			
30	1.112	2.67E – 06	2.67E – 06			
40	1.021	7.38E – 06	7.38E – 06			
50	1.054	8.85E – 06	4.21E – 06			
60	1.043	9.77E – 06	4.57E – 06			
70	0.975	2.14E – 05	5.54E – 06			
80	0.974	3.86E – 05	3.86E – 06			
	Region I			Region II		
	N	A	σ_{dc}	n	A	σ_{dc}
90	0.822	9.13E – 06	1.37E – 04	0.97	2.76E – 05	7.64E – 06
100	0.893	7.20E – 06	1.02E – 04	0.97	2.76E – 05	9.05E – 06
110	0.891	9.31E – 06	1.00E – 04	0.97	2.76E – 05	1.03E – 05
120	0.595	5.69E – 05	5.69E-04	0.89	4.90E – 05	1.83E – 05
130	0.523	1.04E – 04	7.77E – 04	0.87	6.16E – 05	2.31E – 05
140	0.433	2.11E – 04	1.43E – 03	0.82	9.00E – 05	3.37E – 05
150	0.361	2.90E – 04	2.75E – 03	0.78	1.26E – 04	4.72E – 05
160	0.272	5.53E – 04	5.24E – 03	0.71	2.08E – 04	7.80E – 05

It is noticed that the values of the exponent n vary in different salt concentrations [55, 56]. Also, the pure sample has two regions that follow the power law and depend on the frequency range. The change of n in different salt concentrations was attributed to the change in the interface between different constituents of the samples. In the case of polymer blend electrolyte, the host was a polymeric blend beside the remains of the individual polymers (partial miscibility), which did not contribute to the blending process. In this hypothetical region, one can imagine that three contributors are present: the blend electrolyte, the electrolyte solution (remains), and the immiscible remains of PVA and PVP polymers electrolytes.

It is also noted that the behavior of the exponent n at various temperatures of pure blend samples is linear whether at temperatures higher or lower than the glass transition point. At higher temperatures (see Figure 15(b)), two linear regions were detected, and n was linearly dependent on temperature. However, the behavior of n (T) in electrolyte samples follows the exponential function (n decreases exponentially with temperature) [57]. This means that the movement of chains and side chains may be activated due to

Table 4: Values of the exponent n, coefficient A, and the DC conductivity for pure 0.5 wt.% $FeCl_2$ PVA/PVP electrolyte blend sample.

T (°C)	n	A	σ_{dc}
30	1.030	3.52E − 06	3.52E − 05
40	0.878	5.02E − 06	3.52E − 05
50	0.747	7.09E − 06	3.52E − 05
60	0.543	5.38E − 06	2.42E − 04
70	0.400	2.94E − 06	2.47E − 04
80	0.276	2.16E − 03	1.62E − 03
90	0.177	6.35E − 03	4.76E − 03
100	0.124	1.15E − 02	8.62E − 03
110	0.093	1.79E − 02	1.34E − 02
120	0.077	2.52E − 02	1.89E − 02
130	0.062	3.07E − 02	2.30E − 02
140	0.046	4.78E − 02	3.59E − 02

Table 5: Values of the exponent n, coefficient A, and the DC conductivity for pure 1 wt.% $FeCl_2$ PVA/PVP electrolyte blend sample.

T (°C)	n	A	σ_{dc}
30	0.522	1.19E − 03	4.48E − 04
40	0.427	1.09E − 02	4.07E − 03
50	0.245	1.19E − 02	4.44E − 03
60	0.227	1.32E − 02	4.95E − 03
70	0.165	2.22E − 02	8.30E − 03
80	0.082	7.37E − 02	2.76E − 02
90	0.048	9.25E − 02	3.46E − 02
100	0.022	1.17E − 01	4.39E − 02
110	0.012	1.42E − 01	5.30E − 02
120	0.008	1.57E − 01	5.87E − 02
130	0.003	1.56E − 01	5.86E − 02
140	0.002	1.59E − 01	5.94E − 02

Table 6: Values of the exponent n, coefficient A and the dc conductivity for pure 2 wt.% $FeCl_2$ PVA/PVP electrolyte blend sample.

T (°C)	n	A	σ_{dc}
30	0.759	1.35E − 04	2.25E − 05
40	0.594	6.02E − 04	1.00E − 04
50	0.464	1.91E − 03	3.19E − 04
60	0.338	5.72E − 03	9.53E − 04
70	0.202	1.70E − 02	2.83E − 03
80	0.158	2.49E − 02	4.14E − 03
90	0.126	3.52E − 02	5.87E − 03
100	0.087	5.33E − 02	8.88E − 03
110	0.063	7.55E − 02	1.26E − 02
120	0.049	9.72E − 02	1.62E − 02
130	0.041	1.15E − 01	1.91E − 02
140	0.046	1.24E − 01	2.07E − 02

the addition of electrolyte ($FeCl_2$). This will excite the movement of ions significantly and increase their conductivity, as well as this will reduce the effect of interfacial regions, which increase the probability of a hopping mechanism for ions [58]. Also, according to the correlated barrier hopping model (CBH), as the temperature increases, the ionic hopping between sites to overcome the potential barrier will increase [57, 59, 60].

Tables 3–6 illustrate the values of the exponent n, the coefficient A, and the DC conductivity (σ_{dc}) for the pure sample at different temperatures. It is obvious that the increase in the DC conductivity was accompanied by a decrease in the value of n, which means that the plateau region was expanded at the expense of the exponential region of $\sigma(f)$ [56].

These results confirm the role of thermal activation of the main chains beside the side chains that contribute significantly to the electrical conductivity. It is clear that the role of chain movement due to the thermal activation was greater than the role of the applied alternating voltage. The presence of the two pure blend sample regions at high temperatures can be attributed to the presence of more than one conduction mechanism plus the possibility of polymer remains to contribute to a polymer blend.

4. Conclusion

This study investigated some electrical properties of the PVA/PVP polymeric blend as well as its blend electrolyte by adding $FeCl_2$ in different weight percentages (0.5, 1, and 2 wt.%). The incorporation of $FeCl_2$ in the blend matrix enhanced the electrical conductivity of the blend, and the AC conductivity increased as the $FeCl_2$ weight percentage increased. Nyquist plots for pure and blend electrolyte samples demonstrated depressed semicircles at all temperatures. Pure samples did not show a complete semicircle shape due to the insulating nature of the blend and the inability of the charge carriers to move except at high temperatures.

Moreover, the Nyquist plots diameter was reduced as the temperature and/or $FeCl_2$ weight percentage increased, indicating the active participation of the ionic conductivity in the samples. For instance, the AC conductivity was attributed to a hopping mechanism in the pure sample. The results for blend electrolyte samples were interpreted based on the increase of chain mobility due to thermal activation and the contribution of ionic conduction. Jonscher universal power law was applied to study the conduction mechanism in pure and electrolyte blend samples. The activation energy in the blend and blend electrolyte samples was calculated, and the two activation regions appeared in blend electrolyte samples [42].

Data Availability

The data are available from the author upon request.

Disclosure

A preprint has previously been published [56]. This manuscript was presented before on Research Square at the following link: https://www.researchsquare.com/article/rs-204111/v1.

Conflicts of Interest

The author declares that there are no conflicts of interest.

Acknowledgments

This work was supported by the Deanship of Scientific Research (DSR), Vice Presidency for Graduate Studies and Scientific Research, King Faisal University, Saudi Arabia (Project No. GRANT 426).

References

[1] W. Wessel, M. Schoog, and E. J. A. F. Winkler, "Polyvinylpyrrolidone (PVP), its diagnostic, therapeutic and technical application and consequences thereof," *Arznei-mittel-Forschung*, vol. 21, pp. 1468–82, 1971.

[2] C. Pierpaoli, J. Sarlls, U. Nevo, P. Basser, and F. Horkay, "Polyvinylpyrrolidone (PVP) water solutions as isotropic phantoms for diffusion MRI studies," *Proc Intl Soc Magn Reson Med*, vol. 17, p. 1414, 2009.

[3] M. Muthuvinayagam and K. J. H. P. P. Sundaramahalingam, "Characterization of Proton Conducting Poly [ethylene Oxide]: Poly [vinyl Pyrrolidone] Based Polymer Blend Electrolytes for Electrochemical Devices," *High Performance Polymers*, vol. 33, 2020.

[4] S. A. Soud, B. A. Hasoon, A. I. Abdulwahab, N. N. Hussein, and R. K. J. E. J. O. B. Maeh, "Synthesis and characterization of plant extracts loaded PVA/PVP blend films and evaluate their biological activities," *Eurasian Journal of Biosciences*, vol. 14, pp. 2921–2931, 2020.

[5] H. A. Ravin, A. M. Seligman, and J. J. N. E. J. O. M. Fine, "Polyvinyl pyrrolidone as a plasma expander," *New England Journal of Medicine*, vol. 247, no. 24, pp. 921–929, 1952.

[6] S. K. Joneja, W. W. Harcum, G. W. Skinner, P. E. Barnum, and J.-H. J. D. d. Guo, "Investigating the fundamental effects of binders on pharmaceutical tablet performance," *Drug Development and Industrial Pharmacy*, vol. 25, no. 10, pp. 1129–1135, 1999.

[7] M. Kurakula and G. Rao, "Type of Article: REVIEW Pharmaceutical Assessment of Polyvinylpyrrolidone (PVP): As Excipient from Conventional to Controlled Delivery Systems with a Spotlight on COVID-19 Inhibition," *Journal of Drug Delivery Science and Technology*, Article ID 102046, 2020.

[8] M. A. Tofighy, T. Mohammadi, and M. Sadeghi, *High-flux PVDF/PVP Nanocomposite Ultrafiltration Membrane Incorporated with Graphene Oxide Nanoribbones with Improved Antifouling Properties*, vol. 60, Article ID 49718, 2020.

[9] S. Suganthi, S. Vignesh, J. K. Sundar, and V. Raj, "Fabrication of PVA polymer films with improved antibacterial activity by fine-tuning via organic acids for food packaging applications," *Applied Water Science*, vol. 10, no. 4, p. 100, 2020.

[10] Y. Hussein, E. M. El-Fakharany, E. A. Kamoun et al., "Electrospun PVA/hyaluronic acid/L-arginine nanofibers for wound healing applications: nanofibers optimization and in vitro bioevaluation," *International Journal of Biological Macromolecules*, vol. 164, pp. 667–676, 2020.

[11] K. Pavithra, S. Gurumurthy, M. Yashoda et al., "Polymer-dispersant-stabilized Ag nanofluids for heat transfer applications," *J Therm Anal Calorim*, vol. 146, pp. 1–10, 2020.

[12] A. Rasool, S. Ata, and A. J. C. P. Islam, "Stimuli responsive biopolymer (chitosan) based blend hydrogels for wound healing application," *Carbohydrate Polymers*, vol. 203, pp. 423–429, 2019.

[13] R. Alipour, A. Khorshidi, A. F. Shojaei, F. Mashayekhi, and M. J. M. J. P. T. Moghaddam, "Skin wound healing acceleration by Ag nanoparticles embedded in PVA/PVP/Pectin/Mafenide acetate composite nanofibers," *Polymer Testing*, vol. 79, Article ID 106022, 2019.

[14] I. Uslu, S. Keskin, A. Gül, T. C. Karabulut, and M. L. J. H. J. B. C. Aksu, "Preparation and properties of electrospun poly (vinyl alcohol) blended hybrid polymer with aloe vera and HPMC as wound dressing," *Hacettepe Journal of Biology and Chemistry*, vol. 38, pp. 19–25, 2010.

[15] U. M. Subramanian, S. V. Kumar, N. Nagiah, U. T. J. I. J. O. P. M. Sivagnanam, and P. Biomaterials, "Fabrication of polyvinyl alcohol-polyvinylpyrrolidone blend scaffolds via electrospinning for tissue engineering applications," *International Journal of Polymeric Materials and Polymeric Biomaterials*, vol. 63, no. 9, pp. 476–485, 2014.

[16] B. Patel, *Characterisation of Chitosan/PVA/PVP Crossed-Linked Nanofibrous Scaffolds for the Potential Application in Dermal Tissue Engineering*, University of Otago, Dunedin, New Zealand, 2020.

[17] R. M. L. Helberg, Z. Dai, L. Ansaloni, and L. J. G. E. Deng, "PVA/PVP blend polymer matrix for hosting carriers in facilitated transport membranes: synergistic enhancement of CO2 separation performance," *Green Energy & Environment*, vol. 5, no. 1, pp. 59–68, 2020.

[18] F. Oustadi, M. Haghbin Nazarpak, M. Mansouri, F. J. I. J. O. P. M. Ketabat, and P. Biomaterials, "Preparation, characterization, and drug release study of ibuprofen-loaded poly (vinyl alcohol)/poly (vinyl pyrrolidone) bilayer antibacterial membrane," *International Journal of Polymeric Materials and Polymeric Biomaterials*, vol. 71, pp. 1–10, 2020.

[19] J. Chen, X. Cui, Y. Zhu, W. Jiang, and K. J. C. Sui, "Design of superior conductive polymer composite with precisely controlling carbon nanotubes at the interface of a co-continuous polymer blend via a balance of π-π interactions and dipole-dipole interactions," *Carbon*, vol. 114, pp. 441–448, 2017.

[20] H. A. Sallal, A. A. A. Hamead, and F. M. J. D. T. Othman, "Effect of nano powder (Al2O3-CaO) addition on the mechanical properties of the polymer blend matrix composite," *Defence Technology*, vol. 16, no. 2, pp. 425–431, 2020.

[21] Y. Alibwaini, O. Hemeda, R. El-Shater et al., "Synthesis, characterizations, optical and photoluminescence properties of polymer blend PVA/PEG films doped eosin," *Y (EY) dye*, vol. 111, Article ID 110600, 2021.

[22] H. Xu, M. Qu, Q. Yang, and D. W. J. J. O. P. E. Schubert, "Investigating the Electrical Percolation Threshold of Ternary Composite Films with Different Compatibility between Polymer Blends," *journal Journal of Polymer Engineering*, vol. 41, 2021.

[23] F. Ali, R. Kershi, M. Sayed, and Y. J. P. B. C. M. AbouDeif, "Evaluation of structural and optical properties of Ce3+ ions doped (PVA/PVP) composite films for new organic semiconductors," *Physica B: Condensed Matter*, vol. 538, pp. 160–166, 2018.

[24] Y. Tassanapukdee, P. Prayongpan, and K. J. E. T. Songsrirote, "Innovation Removal of heavy metal ions from an aqueous solution by CS/PVA/PVP composite hydrogel synthesized using microwaved-assisted irradiation," *Environmental Technology & Innovation*, vol. 24, Article ID 101898, 2021.

[25] M. A. E. Kader, M. Elabbasy, M. Ahmed, and A. J. J. O. M. R. Menazea, "Structural, morphological features, and antibacterial behavior of PVA/PVP polymeric blends doped with silver nanoparticles via pulsed laser ablation," *Journal of Materials Research and Technology*, vol. 13, pp. 291–300, 2021.

[26] R. Ma, D. Xiong, F. Miao, J. Zhang, and Y. J. M. S. Peng, "Novel PVP/PVA hydrogels for articular cartilage

replacement," *Materials Science and Engineering: C*, vol. 29, no. 6, pp. 1979–1983, 2009.

[27] J. W. J. E. o. A. C. A. Schultz, "Theory and instrumentation," *Dielectric spectroscopy in analysis of polymers*, Wiley, Hoboken, NJ, U.S.A, 2006.

[28] A. Y. Yassin, "Dielectric spectroscopy characterization of relaxation in composite based on (PVA–PVP) blend for nickel–cadmium batteries," *Journal of Materials Science: Materials in Electronics*, vol. 31, no. 21, pp. 19447–19463, 2020.

[29] H. M. Ragab, "Spectroscopic investigations and electrical properties of PVA/PVP blend filled with different concentrations of nickel chloride," *Physica B: Condensed Matter*, vol. 406, no. 20, pp. 3759–3767, 2011/10/15/2011.

[30] F. F. Awang, M. F. Hassan, and K. H. Kamarudin, "Study on ionic conductivity, dielectric and electrochemical properties of solid polymer electrolyte for battery applications," *Ionics*, vol. 28, no. 3, pp. 1249–1263, 2022.

[31] G. Veena and B. Lobo, "Microstructural features, spectroscopic study and thermal analysis of potassium permanganate filled PVA–PVP blend films," *Journal of Physics: Condensed Matter*, vol. 33, no. 25, 2021.

[32] A. Yassin, "Impedance, structural and thermal analyses of polyvinyl alcohol/polyvinyl pyrrolidone blend incorporated with Li+ ions for lithium-ion batteries," *Journal of Materials Research and Technology*, vol. 15, pp. 754–767, 2021.

[33] A. Badawi, S. S. Alharthi, A. A. Alotaibi, and M. G. Althobaiti, "Investigation of the mechanical and electrical properties of SnS filled PVP/PVA polymeric composite blends," *Journal of Polymer Research*, vol. 28, no. 6, p. 205, 2021.

[34] M. Irfan, A. Manjunath, S. S. Mahesh, R. Somashekar, and T. Demappa, "Influence of NaF salt doping on electrical and optical properties of PVA/PVP polymer blend electrolyte films for battery application," *Journal of Materials Science: Materials in Electronics*, vol. 32, no. 5, pp. 5520–5537, 2021.

[35] M. Premalatha, N. Vijaya, S. Selvasekarapandian, and S. Selvalakshmi, "Characterization of blend polymer PVA-PVP complexed with ammonium thiocyanate," *Ionics*, vol. 22, no. 8, pp. 1299–1310, 2016.

[36] N. A. M. Saleh and D. S. A. Salman, "Thermal properties of manganese chloride salt reinforced [PVA: PVP] blend films," *NeuroQuantology*, vol. 19, no. 9, pp. 126–131, 2021.

[37] I. S. Elashmawi and A. A. J. J. O. M. R. Menazea, "Different time's Nd:YAG laser-irradiated PVA/Ag nanocomposites: structural, optical, and electrical characterization," *Journal of Materials Research and Technology*, vol. 8, no. 2, pp. 1944–1951, 2019.

[38] H. Rahmani, S. H. Mahmoudi Najafi, A. Ashori, M. Arab Fashapoyeh, F. Aziz Mohseni, and S. J. C. p. Torkaman, "Preparation of chitosan-based composites with urethane cross linkage and evaluation of their properties for using as wound healing dressing," *Carbohydrate Polymers*, vol. 230, Article ID 115606, 2020.

[39] E. Abdelrazek, I. Elashmawi, and S. J. P. B. C. M. Labeeb, "Chitosan filler effects on the experimental characterization, spectroscopic investigation and thermal studies of PVA/PVP blend films," *Physica B: Condensed Matter*, vol. 405, no. 8, pp. 2021–2027, 2010.

[40] I. Omkaram, R. S. Chakradhar, and J. Lakshmana Rao, "EPR, optical, infrared and Raman studies of VO2+ ions in polyvinylalcohol films," *Physica B: Condensed Matter*, vol. 388, no. 1-2, pp. 318–325, 2007.

[41] M. Głąb, S. K. Kramarczyk, A. Drabczyk et al., "Hydroxyapatite obtained via the wet precipitation method and PVP/PVA matrix as components of polymer-ceramic composites for biomedical applications," *Molecules*, vol. 26, no. 14, p. 4268, 2021.

[42] K. Sundaramahalingam, M. Muthuvinayagam, N. Nallamuthu, D. Vanitha, and M. Vahini, "Investigations on lithium acetate-doped PVA/PVP solid polymer blend electrolytes," *Polymer Bulletin*, vol. 76, no. 11, pp. 5577–5602, 2019.

[43] A. Waly, A. Abdelghany, and A. J. J. O. M. R. Tarabiah, "Study the structure of selenium modified polyethylene oxide/polyvinyl alcohol (PEO/PVA) polymer blend," *Journal of Materials Research and Technology*, vol. 14, pp. 2962–2969, 2021.

[44] H. M. Zidan, E. M. Abdelrazek, A. M. Abdelghany, and A. E. J. J. O. M. R. Tarabiah, "Characterization and some physical studies of PVA/PVP filled with MWCNTs," *Journal of Materials Research and Technology*, vol. 8, no. 1, pp. 904–913, 2019.

[45] K. Li, D. Wang, K. Zhao, K. Song, and J. J. T. Liang, "Electrohydrodynamic jet 3D printing of PCL/PVP composite scaffold for cell culture," *Talanta*, vol. 211, Article ID 120750, 2020.

[46] N. Shahi, G. Joshi, and B. J. P. Min, "Effect of regenerated cellulose fibers derived from black oat on functional properties of PVA-based biocomposite film," *Processes*, vol. 8, no. 9, p. 1149, 2020.

[47] A. Menazea, A. Ismail, N. S. Awwad, and H. A. J. J. O. M. R. Ibrahium, "Physical characterization and antibacterial activity of PVA/Chitosan matrix doped by selenium nanoparticles prepared via one-pot laser ablation route," *Journal of Materials Research and Technology*, vol. 9, no. 5, pp. 9598–9606, 2020.

[48] M. P. Muresan, K. Magyari, and A. Vulpoi, "PVA and PVP hydrogel blends for wound dressing: synthesis and characterisation," in *Advanced Materials Research*, vol. 1151, pp. 9–14, Trans Tech Publications Ltd, Freienbach, Switzerland, 2019.

[49] S.-K. Kim, M. Miyayama, and H. J. J. o. t. C. S. o. J. Yanagida, "Complex impedance and modulus analysis on electrical anisotropy of layer-structured BaBi4Ti4O15 single crystal in paraelectric phase," *Journal of the Ceramic Society of Japan*, vol. 103, no. 1195, pp. 315–318, 1995.

[50] B. Chowdari and S. Radhakrishna, *Solid State Ionic Devices: International Seminar*, World Scientific, Singapore, 1988.

[51] P. Vasudevan, S. Thomas, K. Arunkumar, S. Karthika, and N. Unnikrishnan, "Synthesis and dielectric studies of poly (vinyl pyrrolidone)/titanium dioxide nanocomposites," in *Proceedings of the IOP Conference Series: Materials Science and Engineering*, Kerala, India, February 2015.

[52] J. Bisquert and G. J. R. J. o. E. Garcia-Belmonte, "Interpretation of AC conductivity of lightly doped conducting polymers in terms of hopping conduction," *Russian Journal of Electrochemistry*, vol. 40, no. 3, pp. 352–358, 2004.

[53] A. Jonscher and J. Ak, *The Universal Dielectric Response: A Review of Data and Their New Interpretation*, Chelsea Dielectrics Group, London, U.K, 1980.

[54] S. J. S. S. I. Elliott, "Frequency-dependent conductivity in ionic glasses: a possible model," *Solid State Ionics*, vol. 27, no. 3, pp. 131–149, 1988.

[55] A. H. Mohamad, O. G. Abdullah, and S. R. J. R. i. P. Saeed, "Effect of very fine nanoparticle and temperature on the electric and dielectric properties of MC-PbS polymer nanocomposite films," *Results in Physics*, vol. 16, Article ID 102898, 2020.

[56] S. Hegde, V. Ravindrachary, S. D. Praveena, I. Ismayil, B. Guruswamy, and R. N. Sagar, "Microstructural, dielectric, and transport properties of proton-conducting solid polymer electrolyte for battery applications," *Ionics*, vol. 26, no. 5, pp. 2379–2394, 2020/05/01 2020.

[57] M. A. M. Saeed and O. G. J. M. Abdullah, "Effect of high ammonium salt concentration and temperature on the structure, morphology, and ionic conductivity of proton-conductor solid polymer electrolytes based PVA," *Membranes*, vol. 10, p. 262, 2020.

[58] S. B. Aziz, R. M. Abdullah, M. A. Rasheed, and H. M. J. P. Ahmed, "Role of ion dissociation on DC conductivity and silver nanoparticle formation in PVA: AgNt based polymer electrolytes: deep insights to ion transport mechanism," *Polymers*, vol. 9, no. 12, p. 338, 2017.

[59] S. B. Aziz, O. G. Abdullah, S. R. Saeed, and H. M. J. I. J. E. S. Ahmed, "Electrical and dielectric properties of copper ion conducting solid polymer electrolytes based on chitosan: CBH model for ion transport mechanism," *International Journal of Electrochemical Science*, vol. 13, pp. 3812–3826, 2018.

[60] S. B. Aziz, S. Al-Zangana, H. J. Woo, M. F. Z. Kadir, and O. G. J. R. i. P. Abdullah, "The compatibility of chitosan with divalent salts over monovalent salts for the preparation of solid polymer electrolytes," *Results in Physics*, vol. 11, pp. 826–836, 2018.